INTERNATIONAL JOURNAL OF PRECISION ENGINEERING AND MANUFACTURING Vol. 18, No. 10, pp. 1455-1462 OCTOBER 2017 / 1455

REGULAR PAPER

DOI: 10.1007/s12541-017-0173-6
ISSN 2234-7593 (Print) / 2005-4602 (Online)

The Case Study of Masticatory Force with Food from Full Skull and Partial Model

Yeo-Kyeong Lee[1], Hee-Sun Kim[1], and Jae-Yong Park[1,#]

1 Department of Architectural Engineering, Ewha Womans University, 52, Ewhayeodae-gil, Seodaemun-gu, Seoul, 03760, South Korea
Corresponding Author / E-mail: jypark1212@ewha.ac.kr, TEL: +82-2-3277-2446, FAX: +82-2-3277-6875

KEYWORDS: Masticatory force, Occlusal force, Finite element analysis, Cranium, Maxilla, Mandible

The aim of this paper was to investigate structural and mechanical behavior of mastication of skull with food. Full skull model was performed by rotational displacement control whereas the partial model was performed by linear displacement control in each case of (a) No food and (b) Food. FE models of full skull model and partial model were generated based on CT images. Material properties for teeth, PDL, cortical bone, and cancellous bone were applied to the corresponding parts. Based on the analyses of full skull model, von Mises stress distributions and max. strain distribution were obtained and compared to experimental data for validation of modeling approaches. The stress distribution by occlusal force was propagated to the body of mandible for (a) No food and (b) Food. It was also propagated to the maxilla, nasal bone, frontal bone, zygomatic bone, and temporal bone. The tendency of stress and strain distribution from teeth to maxilla and mandible could be identified to be compared with different experiment. The suggested FE procedure could be used to evaluate structural and mechanical behavior of skull with the full skull model and partial model effectively.

Manuscript received: April 11, 2017 / Revised: June 2, 2017 / Accepted: June 11, 2017

1. Introduction

Finite element analysis (FEA) and design optimization for understanding human body from a mechanical view point have been widely researched in biomedical and biomechanics fields[1-15] over 10 years. The structural behavior of human body can be predicted accurately by experiments since they can be used to diagnose diseases or to design prosthetic devices.[16-23] Accordingly, FEA to simulate behaviors of the human body can be used for the difficulties of measurement of stresses and strains of teeth mastication and skull *in vivo* experiments.

The FE modeling approaches have also been developed to investigate the mechanical behavior of occlusal adjustment and contacts. Oliveira et al.[6] evaluated the effect of different occlusal contact patterns on tooth displacement in an adult dentition using a three-dimensional FE model of human maxilla and mandible. Kasai et al.[13] investigated the influence of occlusal forces exerted during occlusal adjustment on the distribution of forces among teeth and implants in intercuspal clenching using FEA. Eraslan et al.[7] evaluated the effect of different restoration alternatives on stress distributions on endodontically treated teeth without lingual cusp. They found that different restoration techniques did not affect the stress distribution within tooth-restoration complex.

Studies of analytical approaches have been concerned predominantly with the mechanical behavior of the human skull. Kim et al.[24] and Merdji et al.[25] investigated FEA techniques to find the mechanical behavior of mandible bone and single molar tooth, respectively. In particular, Kim et al.[24] proposed an efficient FE modeling technique for predicting stress distributions on mandible under masticatory force. Mandible and teeth without maxilla based computed tomography (CT) images of human skull were modelled on FE. The FEA procedure[24] which was compared analytical results with experimental data could predict the mechanical behavior of mandible and mandibular teeth during mastication with high accuracy. Merdji et al.[25] carried out stress FE analysis of a single molar tooth. They applied FE modeling approach for stress distributions in constituent parts associated with masticatory action in biomechanical research successfully. They also showed that distal-mesial directional loading caused higher von Mises stresses on tooth, periodontal ligament, and cortical bone compared to other directional loads, such as coronal-apical and lingual-buccal directional loads.

Kim et al.[26] suggested CAE procedure of structural analysis to simulate masticatory actions and to predict stress distributions occurring on maxilla, teeth and mandible during mastication with the actual human CT images. Their suggested CAE procedure could variously evaluate the structural and mechanical behaviors of part of maxilla, mandible and teeth.

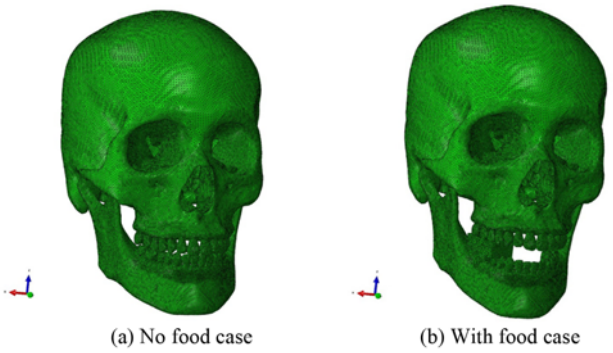

Fig. 1 Full skull FE models

Although many studies simulating masticatory action using FEA have been performed, relatively few analytical studies have been reported about the stress distributions and propagations considering the directions of masticatory action and occlusal force in a real situation. In addition, limitations have been found such that simplified FE models were used without considering the interactive behaviors between maxilla, mandible, and number of teeth. Accordingly, the purposes of this study were to compare mastication action of full skull and partial model with food or not and to predict stress and strain distributions occurring on full skull and partial model during occlusal force is applied. To achieve these goals, FE models of the actual human skull were generated using CT images with food or not. Full skull FE model was used to validate the proposed CAE procedure by comparing the analysis results with the experimental data. Full skull FE model with food was approved the feasibility of suggested CAE procedure. By applying the rotational displacement control as occlusal force in the FE models, the effects on stress and strain distributions of masticatory directions were well investigated. For the cost of full skull FE analysis to reduce, it was used to generate partial FE models with 10 teeth having part of maxilla and mandible to verify the effectiveness of FE analysis with food or not.

2. Analytical Approach

2.1 Finite element model generation[26]

CT (SOMATOMTM SENSATION, Siemens AG, Germany, 120 kVp, 200 ms, 0.75 mm thickness) images were captured from a 38 year old male skull with normal occlusion status and a total of 964 dicom files were obtained. Based on the files, 3-dimensional full skull FE model was generated as illustrated in Fig. 1(a). In order to generate other full skull model including food model, the mandible was moved downward and a rectangular parallelepiped model was applied between right side of maxilla and mandible (Fig. 1(b)). The size of food model was 18 mm × 32 mm × 10 mm (width × length × height). 4-noded tetrahedral elements were used and the element had a degree of freedom in anterio-superior, axial, and anterio-posterior direction at each node. Stress and strain at each direction were calculated at a single integration point per element. The differences of each full skull FE models for (a) No food case and (b) With food case were the distance between upper and lower teeth and the addition of food between upper and lower teeth in (b) With food case. When the food was inserted between upper and lower teeth, the mandible was rotated downward around two point of top of both side condyles. The size and number of elements were tabulated in Table 1.

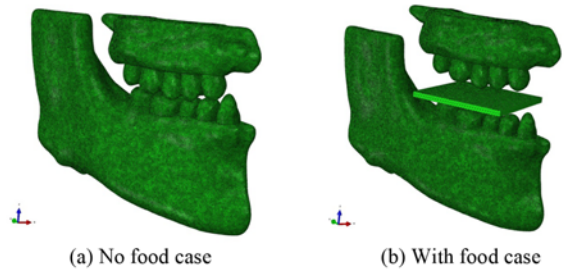

Fig. 2 Partial FE models

Table 1 Size and number of elements of each model

FE models	Size of elements (mm)	No. of elements
Full skull model	0.2-3	3,356,082
Full skull model with food	0.2-3	3,422,865
Food (Full skull model)	0.4-3.5	67,783
Partial model	0.2-0.4	2,433,406
Partial model with food	0.2-0.4	2,447,326
Food (Partial model)	0.8-1.2	13,920

Table 2 Material properties used in the models[25]

Parts	Elastic modulus (GPa)	Poisson's ratio
Molar tooth	20	0.3
Periodontal ligament (PDL)	0.005	0.49
TMJ	10	0.3
Cortical bone	14.5	0.323
Cancellous bone	1.37	0.3
Food	0.0002	0.49

For simplification of the analytical process, partial FE models were considered. The partial models contained a part of right maxilla and mandible, and 5 upper and 5 lower teeth as shown in Fig. 2. In case of the partial model with food, the size of food was 31 mm × 31 mm × 1.6 mm (width × length × height) according to the distance between upper and lower teeth. Since this study assumed that stress distribution of food was not important, the food size was selected arbitrarily. The partial models also used 4-noded tetrahedral elements and the size and number of elements were listed in Table 1.

The full skull models had 4 or 5 parts; teeth, periodontal ligament (PDL), cortical bone, cancellous bone, temporomandibular joint (TMJ) and/or food. The interfaces between teeth and PDL, as well as cortical bone and cancellous bone were treated as perfect bond. Furthermore, the effect of PDL was considered by adding tied contact formulations on the interface between PDL and mandibular bone. The formulations were used to save computational time. However, PDL and cancellous bone were very fine and soft parts so that there were lots of numerical issue in analyses. Therefore, they were neglected in the partial models and the models had only 2 or 3 parts; teeth, cortical bone, and/or food. Each part was modeled with corresponding elastic modulus and Poisson's ratio referred to previously reported data as listed in Table 2.

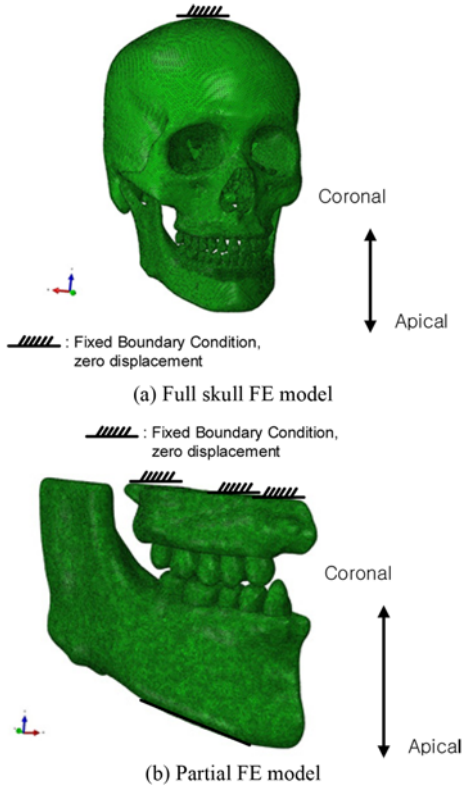

Fig. 3 Loading and restraint prescriptions of each model

Especially, material properties of dentin were applied to teeth models only, because the enamel and cementum could be assimilated into the volume of the dentin.[16-20] Linear elastic material behaviors were used since this study assumed that stresses on maxilla, teeth and mandible would not undergo their elastic limit during the masticatory simulation. For food model, material properties of beef jerky were applied according to the previous study[27] about the masticatory experiment.

2.2 Boundary conditions

For masticatory simulation, loading and restraint prescriptions were applied as illustrated in Fig. 3. There were three directional movements for mastication; coronal-apical, mesial-distal, and buccal-lingual directional movements. In this study, only coronal-apical directional force was defined as the masticatory force. Loading was prescribed in form of displacement control and rotational-displacement was applied in case of full skull FE model. Parametric study results showed that rotational-displacement was more reasonable than translational-displacement. For instance, stress at tegmen tympani was too excessive when the translational-displacement was applied. In addition, the mandible rotated on the condyle contact surface and TMJ in real mastication. To generate rotational-displacement, one point at mid of the mandible surface was selected. Considering distance between the point and rotational axis, the point was moved 8mm into z-direction and 6.45mm into y-direction, simultaneously. Restraint conditions were prescribed at the top area of bregma in order to prevent collapse of the model during mandible movement. This is because over stress was appeared at the area of foramen magnum when cervical vertebrae was restrained, though skull was supported by cervical vertebrae.

In case of partial FE model in Fig. 3(b), translational-displacement was applied for masticatory simulation to simplify analytical details. The part of mandible was moved 5 mm into z-direction only. Points of cranium part around bregma were fixed all directions (x, y, z), because the skull was moved backward when the FE analysis was accomplished to select points around the foramen magnum. Contact formulation was included between upper and lower teeth with friction coefficient of 0.2 referred to the previous study.[27]

3. Validation of Analytical Model

To compare with experimental results for validation, material properties of replica skull were applied to the analysis. Teeth, cortical bone and cancellous bone were modeled with photopolymer resin (TSR-821, E = 2.5 GPa, ν = 0.3), and PDL and TMJ were modeled with silicone impression (Examix Fine, GC, E = 1.0417 MPa, ν = 0.375). Linear elastic material behavior was considered since this study assumed that stresses on each part would not undergo their elastic limit during the masticatory simulation.

3.1 Boundary conditions

In order to generate effective masticatory simulation, loading and restraint conditions were considered. Loading was prescribed in form of displacement control. Parametric study was performed to determine loading point and displacement control method. It showed that rotational-displacement was more reasonable, because stress on auditory meatus was too excessive when translational-displacement was applied. For rotational-displacement, one point at mid of mandible surface was selected. Measuring distance between the point and rotational axis, the point was moved 5 mm into z-direction and 3.737 mm into y-direction, simultaneously. Restraint conditions were prescribed around foramen magnum, because this skull model did not have cervical vertebrae which supported and connected skull to body. All directions (x, y, z) were fixed to prevent toppling the model during mandible movement. Interfaces between teeth and PDL, PDL and cancellous bone, also cortical bone and cancellous bone were treated as perfect bond. In addition, tied-contact formulation was included on the interface between TMJ and upper or lower condyle, respectively so that cranium and mandible were connected. Sliding formulation was applied between upper and lower teeth with friction coefficient of 0.2 referred to the previous study.[27] Linear geometrical analysis was performed using commercial software ABAQUS version 6.10-3 (Dassault Systèmes, Vélizy-Villacoublay, France).

3.2 Analytical results

As illustrated in Fig. 4, stress was propagated from occlusal surface of teeth to alveolar bone. The stress was distributed to maxilla; nasal bone, frontal bone, zygomatic bone, and temporal bone. Stress in maxilla and frontal bone was relatively low, while high stress was found in temporal bone contacted with condyle of mandible. In addition, the stress was concentrated at condyle and ramus of mandible and stress at pterygopalatine suture was higher due to stress in the maxillary. The stress distribution was also found in capsular of temporal bone contacted with condyle of mandible. It was propagated to the temporal bone and

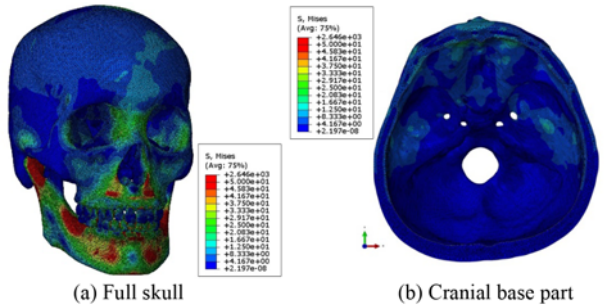

(a) Full skull (b) Cranial base part

Fig. 4 von Mises stress distribution in full skull model

the occipital bone. The stress by occlusal force was propagated to total cranial. High stress distribution was found to be higher at forward of rear cranial and outside of rear middle cranial than stress at front cranial. The stress was found throughout the temporal bone and the sphenoid bone. It was especially found at the condyle of mandible, tegmen tympani of capsular, and backward of jugum of sphenoid bone.

In mandible, the stress distribution by occlusal was propagated at the base of mandible from each teeth to the mandibular body. It was concentrated at backward of second molar of mandible and was reduced from backward to forward in mandible. The stress distribution which was propagated from teeth of mandibular body to backward of mandibular body was concentrated at the head of mandible and the posterior border of ramus. In inferior border of ramus, alveolar part and coronoid process, it was lower than in the posterior border of ramus, the mandibular body and forward of coronoid process. Accordingly, the procedure of FE analysis in full skull FE model was well accomplished in terms of prosthetic dentistry.

3.3 Comparison analytical with experimental results

In order to investigate the feasibility of FE analysis in full skull FE model, the analytical results were validated with the experimental results.[28] Keum fabricated the replica skull model based on the same CT images as this study. The strain gauges were attached at the significant locations from a biomedical perspective. Strain was measured when 100 N and 300 N of occlusal forces were applied using Universal testing machine (UTM) Instron as shown in Fig. 5(a).

As illustrated in Fig. 5(b) and Tables 3, 6 representative locations associated with the mastication were picked as the points for strain measurement. Strain obtained from the experiment and the analysis were compared at each point when 100 N and 300 N of occlusal force were applied.

The analytical results were compared with the experimental results as shown in Table 4. Strain measured in the experiments was 38.028-187.641 μmm/mm when 100 N was applied and it was 130.233-782.548 μmm/mm when 300 N was applied. Similarly, strain obtained from the analysis was 37.422-187.376 μmm/mm in case of occlusal force 100 N and it was 132.799-648.475 μmm/mm in case of occlusal force 300 N. Both experimental and analytical results showed similar tendency that strain at M_2P, FZ and Tza was lower, while strain at M_2B, M_2BA and Or was higher. As illustrated in Fig. 6, error between experimental and analytical results was generally small, but some points such as M_2P and FZ have differences. The differences were predicted by modelling and

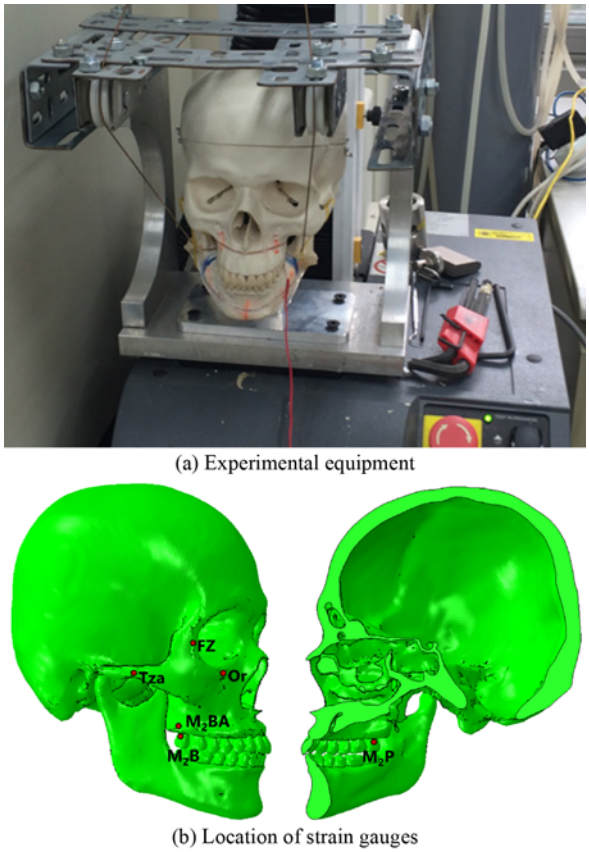

(a) Experimental equipment

(b) Location of strain gauges

Fig. 5 Experimental setup of replica skull with strain gauges

Table 3 Definition of points for strain gauge on skull model

Location	Definition
M_2B	Buccal surface of upper 2nd molar
M_2P	Palatal surface of upper 2nd molar
M_2BA	Buccal alveolar bone on upper 2nd molar apex
FZ	Midpoint of fronto-zygomatic suture on the lateral orbital rim
Or	Lower anterior area on infraorbital margin of the orbit
Tza	Zygomatic process of temporal bone

Table 4 Strains obtained from experiment[28] and analysis (μmm/mm)

Location	Occlusal force 100 N		Occlusal force 300 N	
	Experiment	Analysis	Experiment	Analysis
M_2B	39.104	37.422	130.412	132.799
M_2BA	62.423	63.953	179.747	171.401
M_2P	187.641	187.376	782.548	648.475
FZ	166.471	143.605	658.692	452.105
Or	38.028	49.368	130.233	144.424
Tza	110.679	115.435	390.570	395.575

mesh generation in M_2P and FZ because the points were hard to modelling and mesh generation.

4. Results of Analytical Models with Food

4.1 Full skull model with food

In case of full skull model in Fig. 7, the stress was concentrated at

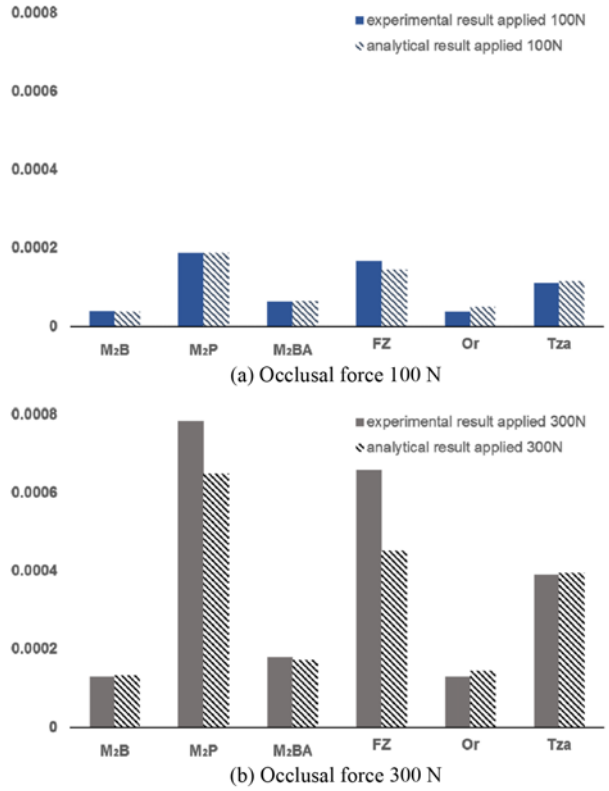

Fig. 6 Histograms of error size between experiment and analysis

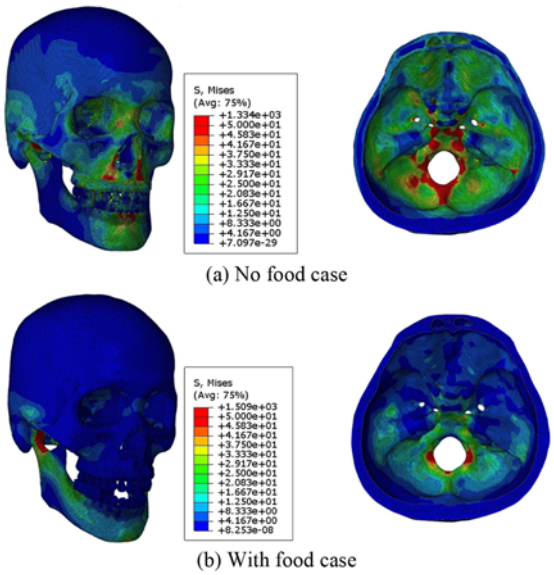

Fig. 7 von Mises stress distribution in full skull and Cranial base

the alveolar bone around mandibular molars and the posterior border of mandibular ramus. It was because food was located at the ramus of mandible. Especially, stress in the alveolar bone around the first and second molar was higher than it of other alveolar part of teeth as shown in Fig. 7(b). Stress was propagated from occlusal surface of teeth to alveolar bone the full skull model without food.

Relatively low stress was found at maxilla, mandible, and frontal bone, while high stress was found at the temporal bone contacted with

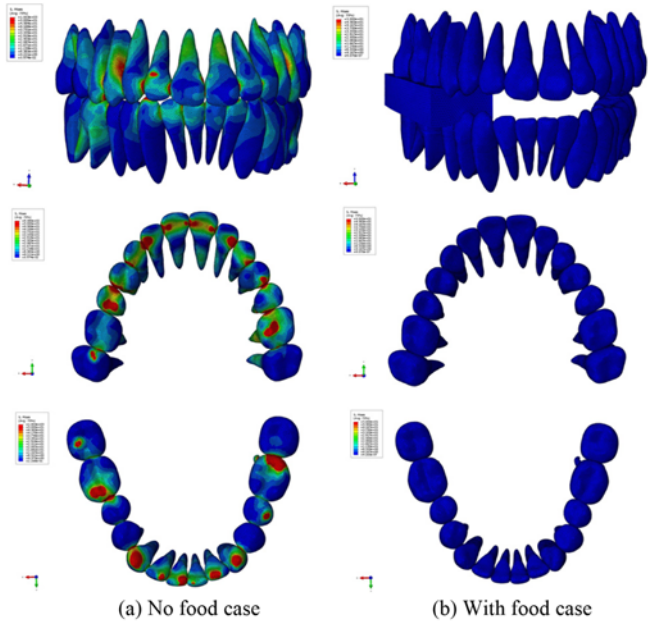

Fig. 8 von Mises stress distribution at teeth in the full skull models in each cases

condyle of mandible and occipital bone. The occlusal force of maxillary was propagated to maxilla, nasal bone, frontal bone, and zygomatic bone. It was found at maxilla above molar which was masticated with zygomatic lower and zygomatic temporal suture and the area of capsular of temporal bone contacted with condyle of mandible. This was propagated at temporal bone and occipital bone.

In the cranial base part, the stress distribution by occlusal force was well propagated. Higher stress distributions of rear outside of middle cranial and forward of rear cranial were found compared to those of the front cranial. Those of prechiasmatic groove of sphenoid bone in (a) No food case was found to be higher than (b) With food case. The stress was distributed throughout the temporal bone and the sphenoid bone. High stress distribution was found at tegmen tympani of capsular and backward of jugum of sphenoid bone especially.

In the mandibular body, it was propagated from downward of molar at the body of mandible to ramus and posterior border of ramus. It was concentrated at the body of mandible. The stress of the condyle of mandible was found to be lower than that of no food case. This was concentrated from the oblique line to the area of posterior border of ramus. The stress was reduced from distal location of body of mandible to mesial location. The stress of alveolar part of mandible was found to be lower than that of ramus.

In case of (a) No food case and (b) With food case in Fig. 8, it was shown that the occlusal force by (a) No food case was evenly distributed across total teeth. In the case of (b) With food case, it is just appeared no. 4, 5, 6, 7 of upper and lower teeth. Molars in the two models was propagated to maxilla, nasal bone frontal bone, zygomatic bone, and temporal bone. The stress distribution in propagation aspects was uniformed in no food case.

4.2 Partial model with food

In case of the partial models, the stress was propagated from teeth

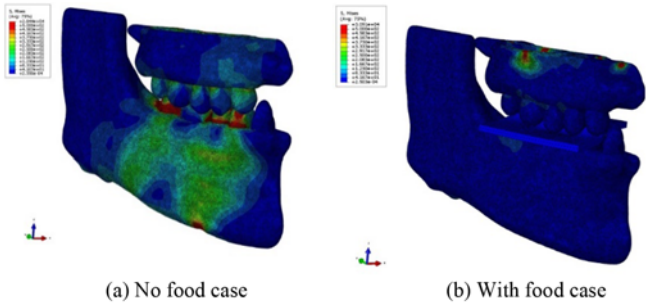

Fig. 9 Stress contours in each cases

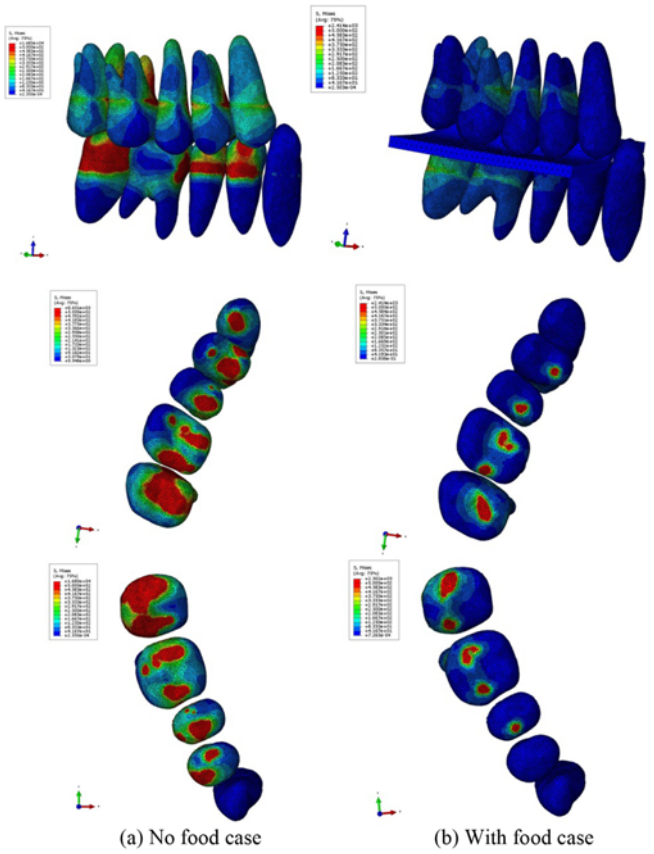

Fig. 10 The distribution of von Mises stress of partial model in each cases

to maxilla and mandible as illustrated in Fig. 9(a) No food case. Occlusal force of maxillary was propagated to maxilla and occlusal force by mandible was propagated to the mandibular body. The stress distribution of mandibular body was concentrated at the base of mandible and body of mandible. Low stress distribution was found in ramus and the posterior border of ramus. High stress distribution was found in the alveolar part. In Fig. 9(b) food case, the stress distribution was propagated from teeth to maxilla and mandible. Occlusal force of maxillary was propagated to maxilla and occlusal force by mandible was propagated to oblique line of mandible. Those of mandibular body was concentrated at the alveolar process of maxilla, the location of horizontal plate of palatine bone, and the location of palatine process of maxilla. Low stress distribution was found in ramus and posterior border of ramus. High stress distribution was also found in alveolar part.

Table 5 Comparison between full skull and partial models

Measuring location of M_1P	von Mises stress (MPa)	Strain (mm/mm)
Full skull - No food case	35.978	$9.78*10^{-4}$
Full skull - Food case	7.047	$2.94*10^{-4}$
Partial model - No food case	35.516	$9.79*10^{-4}$
Partial model - Food case	7.411	$3.42*10^{-4}$

The occlusal surface of teeth by occlusal force and the stress distribution of 10 teeth are shown in Fig. 10. In case of (a) No food case, high stress distribution was found at teeth themselves. It was propagated from a tooth to the next tooth because the interval between a tooth and a tooth was very small when the occlusal force was applied for the surface of teeth. High stress distribution was found at molar typically. There were differences of stress distribution by occlusal force in molars from the first to the third because there were the differences of teeth alignment in each person. It was found at periodontal direction than teeth themselves in (b) Food case because the food was masticated by teeth. The comparison of stress and strain of full skull model and partial model is listed in Table 5. Accordingly, the information obtained by partial model could be analyzed for changed or replaced molar.

5. Conclusions

In this study, a CAE procedure was suggested to predict the mechanical behaviors of full skull during mastication using the rotational displacement conditions and to establish the mechanical behaviors by mastication force using full skull and partial model with food or not. The proposed FE models could evaluate the structural and the mechanical behaviors of cranium, teeth, and mandible effectively even if the models are modified to simulate mastication situations. It was validated that the tendency of stress and strain distribution from teeth to maxilla and mandible can be identified to be compared FE analysis with experiment in full skull model. It was also possible that this procedure predicted mechanical behaviors of mastication with food using full skull and partial models. It was verified that the partial model was sufficient to analyze for the mastication. Accordingly, in order to evaluate the structural and mechanical behavior of the extraction of teeth and the insertion of implant such as small areas, a partial model could be used to obtain results of simulation, thus saving cost of FE analysis.

ACKNOWLEDGMENT

This research was supported by Basic Science Research Program through the National Research Foundation of Korea (NRF) funded by the Ministry of Science, ICT & Future Planning (NRF-2014R1A1A 1007583).

REFERENCES

1. Correia, A., Piloto, P., Campos, J., and Vaz, M., “Finite Element

Analysis of the Mechanical Behavior of a Partially Edentulous Mandible as a Function of Cancellous Bone Density," Journal of Dental Science, Vol. 24, No. 1, pp. 22-27, 2009.

2. Asmussen, E., Peutzfeldt, A., and Sahafi, A., "Finite Element Analysis of Stresses in Endodontically Treated, Dowel-Restored Teeth," The Journal of Prosthetic Dentistry, Vol. 94, No. 4, pp. 321-329, 2005.
3. Baek, S.-H., Cha, H.-S., Cha, J.-Y., Moon, Y.-S., and Sung, S.-J., "Three-Dimensional Finite Element Analysis of the Deformation of the Human Mandible: A Preliminary Study from the Perspective of Orthodontic Mini-Implant Stability," The Korean Journal of Orthodontics, Vol. 42, No. 4, pp. 159-168, 2012.
4. Cruz, M., Wassall, T., Toledo, E. M., da Silva Barra, L. P., and Cruz, S., "Finite Element Stress Analysis of Dental Prostheses Supported by Straight and Angled Implants," International Journal of Oral & Maxillofacial Implants, Vol. 24, No. 3, pp. 391-401, 2009.
5. Daumas, B., Xu, W., and Bronlund, J., "Jaw Mechanism Modeling and Simulation," Mechanism and Machine Theory, Vol. 40, No. 7, pp. 821-833, 2005.
6. Gomes de Oliveira, S., Seraidarian, P., Landre, J., Oliveira, D., and Cavalcanti, B., "Tooth Displacement due to Occlusal Contacts: A Three-Dimensional Finite Element Study," Journal of Oral Rehabilitation, Vol. 33, No. 12, pp. 874-880, 2006.
7. Eraslan, Ö., Eraslan, O., Eskitaşcıoğlu, G., and Belli, S., "Conservative Restoration of Severely Damaged Endodontically Treated Premolar Teeth: A FEM Study," Clinical Oral Investigations, Vol. 15, No. 3, pp. 403-408, 2011.
8. Eser, A., Akca, K., Eckert, S., and Cehreli, M. C., "Nonlinear Finite Element Analysis Versus Ex Vivo Strain Gauge Measurements on Immediately Loaded Implants," International Journal of Oral & Maxillofacial Implants, Vol. 24, No. 3, pp. 439-446, 2009.
9. Fitton, L., Shi, J., Fagan, M., and O'Higgins, P., "Masticatory Loadings and Cranial Deformation in Macaca Fascicularis: A Finite Element Analysis Sensitivity Study," Journal of Anatomy, Vol. 221, No. 1, pp. 55-68, 2012.
10. Hattori, Y., Satoh, C., Kunieda, T., Endoh, R., Hisamatsu, H., and Watanabe, M., "Bite Forces and their Resultants during Forceful Intercuspal Clenching in Humans," Journal of Biomechanics, Vol. 42, No. 10, pp. 1533-1538, 2009.
11. Ichim, I., Swain, M., and Kieser, J., "Mandibular Stiffness in Humans: Numerical Predictions," Journal of Biomechanics, Vol. 39, No. 10, pp. 1903-1913, 2006.
12. Karl, M., Graef, F., Heckmann, S., and Taylor, T., "A Methodology to Study the Effects of Prosthesis Misfit Over Time: An in Vivo Model," International Journal of Oral & Maxillofacial Implants, Vol. 24, No. 4, pp. 689-694, 2009.
13. Kasai, K., Takayama, Y., and Yokoyama, A., "Distribution of Occlusal Forces during Occlusal Adjustment of Dental Implant Prostheses: A Nonlinear Finite Element Analysis Considering the Capacity for Displacement of Opposing Teeth and Implants," International Journal of Oral & Maxillofacial Implants, Vol. 27, No. 2, pp. 329-335, 2012.
14. Harrison, S. M., Eyres, G., Cleary, P. W., Sinnott, M. D., Delahunty, C., and Lundin, L., "Computational Modeling of Food Oral Breakdown Using Smoothed Particle Hydrodynamics," Journal of Texture Studies, Vol. 45, No. 2, pp. 97-109, 2014.
15. Luo, X., Yang, B., Sheng, L., Chen, J., Li, H., et al., "CAD Based Design Sensitivity Analysis and Shape Optimization of Scaffolds for Bio-Root Regeneration in Swine," Biomaterials, Vol. 57, pp. 59-72, 2015.
16. Abraham, C. L., Maas, S. A., Weiss, J. A., Ellis, B. J., Peters, C. L., and Anderson, A. E., "A New Discrete Element Analysis Method for Predicting Hip Joint Contact Stresses," Journal of Biomechanics, Vol. 46, No. 6, pp. 1121-1127, 2013.
17. Yang, H., Nawathe, S., Fields, A. J., and Keaveny, T. M., "Micromechanics of the Human Vertebral Body for Forward Flexion," Journal of Biomechanics, Vol. 45, No. 12, pp. 2142-2148, 2012.
18. Post, A., Hoshizaki, B., and Gilchrist, M. D., "Finite Element Analysis of the Effect of Loading Curve Shape on Brain Injury Predictors," Journal of Biomechanics, Vol. 45, No. 4, pp. 679-683, 2012.
19. Evans, S., Parr, W., Clausen, P., Jones, A., and Wroe, S., "Finite Element Analysis of a Micromechanical Model of Bone and a New 3D Approach to Validation," Journal of Biomechanics, Vol. 45, No. 15, pp. 2702-2705, 2012.
20. Cheng, J., Howard, I. C., and Rennison, M., "Study of an Infant Brain Subjected to Periodic Motion via a Custom Experimental Apparatus Design and Finite Element Modelling," Journal of Biomechanics, Vol. 43, No. 15, pp. 2887-2896, 2010.
21. Yoon, Y. J. and Cowin, S. C., "An Estimate of Anisotropic Poroelastic Constants of an Osteon," Biomechanics and Modeling in Mechanobiology, Vol. 7, No. 1, pp. 13-26, 2008.
22. Yoon, Y. J. and Cowin, S. C., "The Estimated Elastic Constants for a Single Bone Osteonal Lamella," Biomechanics and Modeling in Mechanobiology, Vol. 7, No. 1, pp. 1-11, 2008.
23. Yoon, Y. J., "Estimation of the Elastic Constants of Dentin," Int. J. Precis. Eng. Manuf., Vol. 14, No. 2, pp. 317-322, 2013.
24. Kim, H.-S., Park, J.-Y., Kim, N.-E., Shin, Y.-S., Park, J.-M., and Chun, Y.-S., "Finite Element Modeling Technique for Predicting Mechanical Behaviors on Mandible Bone during Mastication," The Journal of Advanced Prosthodontics, Vol. 4, No. 4, pp. 218-226, 2012.
25. Merdji, A., Mootanah, R., Bouiadjra, B. A. B., Benaissa, A., Aminallah, L., and Mukdadi, S., "Stress Analysis in Single Molar Tooth," Materials Science and Engineering: C, Vol. 33, No. 2, pp. 691-698, 2013.
26. Kim, H.-S., Lee, Y.-K., and Park, J.-Y., "Development of FEA

Procedures for Mechanical Behaviors of Maxilla, Teeth and Mandible," Int. J. Precis. Eng. Manuf., Vol. 17, No. 6, pp. 785-792, 2016.

27. Cho, Y.-E., Park, E.-J., Koak, J.-Y., Kim, S.-K., Heo, S.-J., and Park, J.-M., "Strain Gauge Analysis of Occlusal Forces on Implant Prostheses at Various Occlusal Heights," International Journal of Oral & Maxillofacial Implants, Vol. 29, No. 5, pp. 1034-1041, 2014.

28. Keum, B. K., "Experimental Study for Masticatory Strains on Teeth, Alveolar Bone, Facial Bone, and Cranial Base Foolowing Mesial Position of Maxillary Molars," Ewha Womans University, 2014.